

## High-Resolution Electron and Gamma-Ray Studies and Conversion-Coefficient Measurements in $^{132}\text{Xe}$

H. K. CARTER\* AND J. H. HAMILTON

*Physics Department,† Vanderbilt University, Nashville, Tennessee 37203*

AND

J. C. MANTHURUTHIL AND S. R. AMTEY‡

*Aerospace Research Laboratories,§ Wright Patterson Air Force Base, Dayton, Ohio 45433*

AND

J. J. PINAJIAN

*Oak Ridge National Laboratory,|| Oak Ridge, Tennessee 37830*

AND

E. F. ZGANJAR\*\*

*Department of Physics and Astronomy, Louisiana State University, Baton Rouge, Louisiana 70803*

(Received 23 May 1969)

The  $\gamma$ -ray spectrum from the decay of  $^{132}\text{I}$  was measured with small- and large-volume, high-resolution Ge(Li) detectors, and 116 transitions were assigned in its decay. Selected regions of the conversion-electron spectrum were measured with an iron double-focusing spectrometer. The  $K$ -conversion coefficient of the 772-keV transition that was measured relative to the  $K$ -conversion coefficient of the 662-keV transition in  $^{137}\text{Ba}$  was used to normalize the electron and  $\gamma$  spectra to obtain the  $K$ -conversion coefficients of the 262.7-, 284.7-, 505.9-, 522.6-, 621.0-, 630.2-, 650.6-, 669.8-, 671.5-, 727.1-, 809.8-, 812.3-, 954.6-, 1136.0-, 1143.4-, 1173.2-, 1372.1-, and 1398.6-keV transitions. Conversion coefficients of additional transitions were obtained from electron intensities of other work. From these conversion coefficients, each of the above transitions was assigned an  $M1$  and/or  $E2$  multipolarity.

### I. INTRODUCTION

MEASUREMENTS of internal-conversion-electrons have been made by three groups<sup>1-3</sup> for 16 transitions in the decay of  $^{132}\text{I}$ . These data were combined with  $\gamma$ -ray intensities<sup>2,4,5</sup> obtained from NaI detectors to obtain conversion coefficients for four prominent transitions.<sup>3</sup> The measured  $K$ -conversion coefficient<sup>3</sup> of the 667-keV transition was used to normalize the relative electron and  $\gamma$ -ray intensities. Each of these four transitions was observed to be of  $M1$  and/or  $E2$  multipolarity. A transition of 1143 keV was tentatively assigned<sup>3,6</sup> as  $E1$  from an upper limit of its electron intensity from coincidence studies. The level at 2583.9

keV thus was assigned tentatively a spin and parity of  $3^-$ . The 620-keV transition from this level was thus taken<sup>6</sup> as  $E1$  also.

With the development of high-resolution lithium-drifted germanium detectors Ge(Li), a reinvestigation of the  $^{132}\text{I}$  decay scheme was in order. In particular, relative  $\gamma$ -ray intensities from high-resolution studies in this complex decay would make it possible to obtain conversion coefficients of nine additional transitions for which electron data were known.<sup>1-3</sup> Then, with  $\gamma$ -ray intensities available from high-resolution studies, further conversion-electron measurements were desirable to obtain conversion coefficients for additional transitions. Furthermore, since the 667-keV region is so complex, it was desirable to directly measure another conversion coefficient as a cross check on the normalization. Finally, doublets at 505–507, 650–652, and 727–729 keV observed in electron studies were not observed in  $\gamma$ -ray spectra except for a 729-keV impurity.<sup>7</sup> Thus, additional electron studies of these regions were in order. We have carried out high-resolution  $\gamma$ -ray studies with small- and large-volume Ge(Li) detectors. The  $K$ -conversion coefficient of the 772-keV transition has been measured directly, and additional conversion-electron intensity measurements have been made. The additional electron measurements were made on transitions whose multiplicities would be particularly useful in the assigning of spins and parities to levels. These data were combined to obtain multipolarity assign-

\* Present address: Physics Department, Furman University, Greenville, S.C.

† Work supported in part by a grant from the National Science Foundation.

‡ Working under Air Force Contract No. AF33(615)-1915 with Ohio State University Research Foundation.

§ An element of the Office of Aerospace Research of the U.S. Air Force.

|| Research sponsored by the U.S. Atomic Energy Commission under contract with the Union Carbide Corporation.

\*\* Part of this work performed while this author was at the Materials Testing Reactor, National Reactor Testing Station, Idaho Falls, Id.

<sup>1</sup> J. H. Hamilton, P. F. H. Goudsmit, and J. F. W. Jansen, *Physica* **29**, 885 (1963).

<sup>2</sup> N. R. Johnson, K. Wilsky, P. G. Hansen, and H. L. Nielsen, *Nucl. Phys.* **72**, 617 (1965).

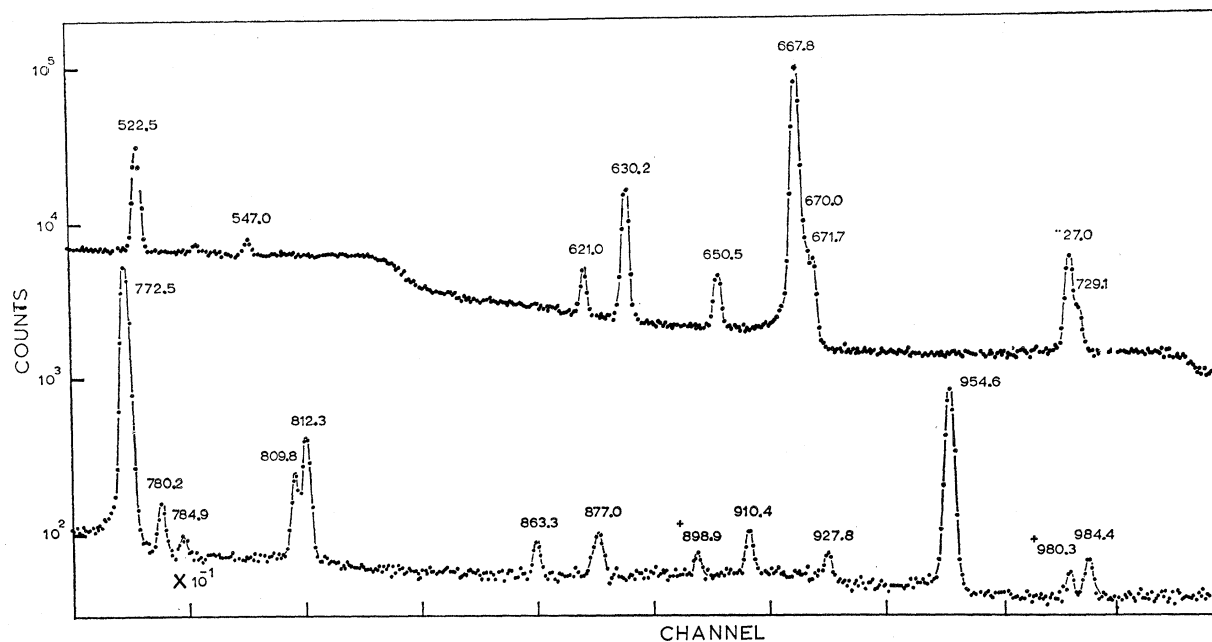
<sup>3</sup> H. W. Boyd and J. H. Hamilton, *Nucl. Phys.* **72**, 604 (1965).

<sup>4</sup> R. L. Robinson, E. Eichler, and N. R. Johnson, *Phys. Rev.* **122**, 1863 (1961).

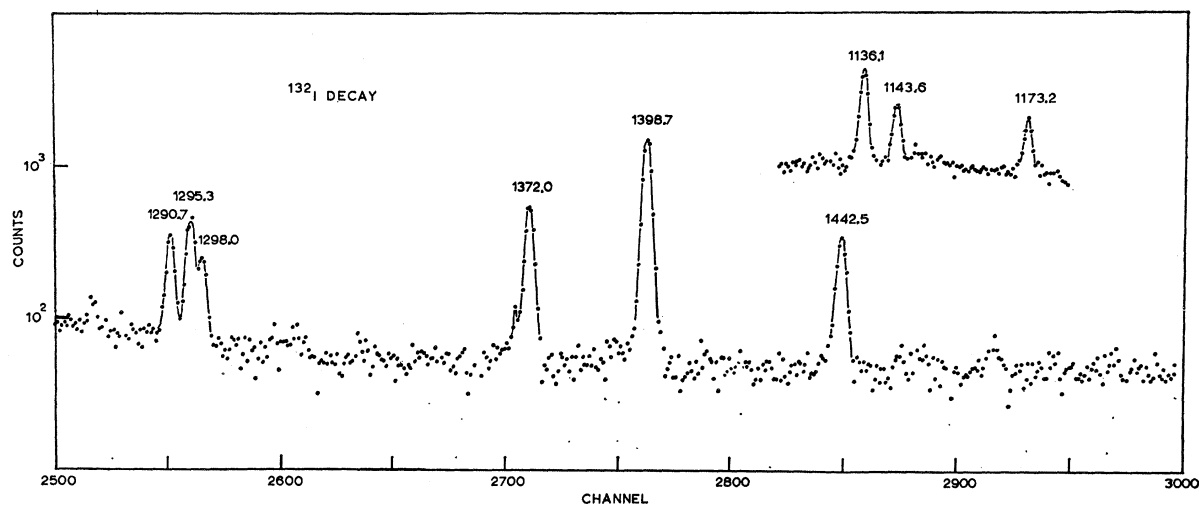
<sup>5</sup> H. G. Devare, *Nucl. Phys.* **28**, 148 (1961).

<sup>6</sup> J. H. Hamilton, H. W. Boyd, and N. R. Johnson, *Nucl. Phys.* **72**, 625 (1965).

<sup>7</sup> J. H. Hamilton, H. K. Carter, and E. F. Zganjar, *Bull. Am. Phys. Soc.* **11**, 775 (1966).



(a)



(b)

FIG. 1.  $\gamma$ -ray singles spectra from the decay of  $^{132}\text{I}$  as taken with a  $^{132}\text{Te}$ - $^{132}\text{I}$  source. These spectra were taken at the Materials Testing Reactor with a 2-cc Ge(Li) detector with cooled preamplifier.

ments for an additional 15 transitions. In the course of these studies, Henck and co-workers<sup>8</sup> reported studies of the lower-energy region of the electron spectrum. Our measurements indicate that all the observed transitions are  $M1$  and/or  $E2$ . Preliminary reports of these studies have appeared elsewhere.<sup>7,9</sup> In the course of these investigations, studies of the  $\gamma$ -ray spectra also

were reported by other groups<sup>10-13</sup> who used Ge(Li) detectors and in one case a pair-spectrometer arrangement. Comparisons with these results yield significant differences in intensities in the higher-energy regions

<sup>8</sup> R. Henck (private communication); M. R. Henck and A. Gizon, *Compt. Rend.* **269**, 337 (1969).

<sup>9</sup> H. K. Carter, J. H. Hamilton, S. R. Amtey, J. C. Manthuruthil, and J. J. Pinajian, *Bull. Am. Phys. Soc.* **13**, 1466 (1968).

<sup>10</sup> R. Henck, L. Stab, P. Siffert, and A. Coche, *Nucl. Phys.* **A93**, 597 (1967).

<sup>11</sup> G. Ardisson and F. X. Petit, *Compt. Rend.* **263C**, 1408 (1966).

<sup>12</sup> C. Ythier, G. Ardisson, and M. Lefort, *Compt. Rend.* **264B**, 84 (1967).

<sup>13</sup> R. Gunnink (private communication to N. R. Johnson and J. H. Hamilton).

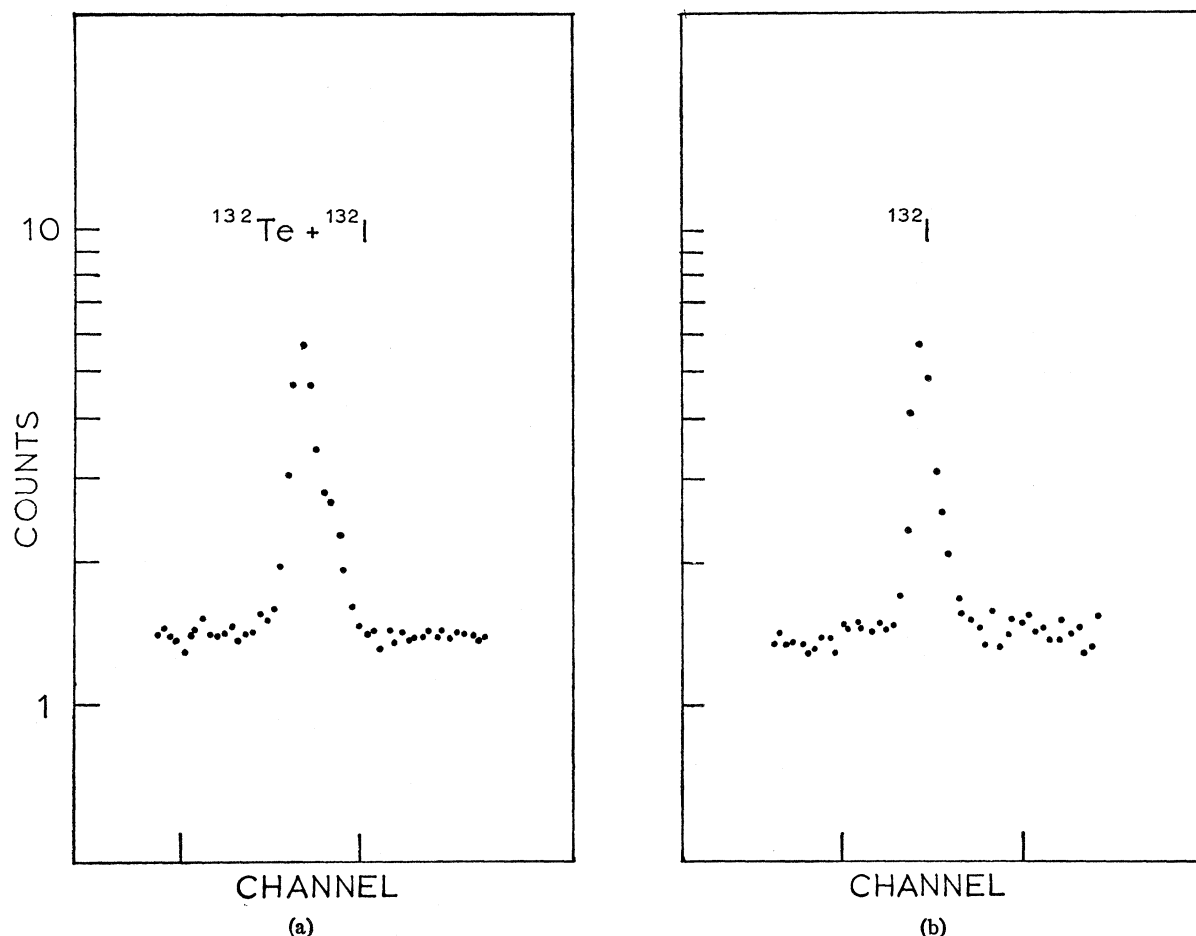


FIG. 2.  $\gamma$ -ray spectra of the 727–729-keV region of  $^{132}\text{I}$  taken with sources of  $^{132}\text{Te}$  in equilibrium with  $^{132}\text{I}$  and separated  $^{132}\text{I}$ . The spectra on the left shows clearly that the 729-keV transition is primarily a contaminant in  $^{132}\text{I}$ .

in some cases. Coincidence studies and the level structure of  $^{132}\text{I}$  are discussed in detail in the following paper.<sup>14</sup>

## II. EXPERIMENTAL PROCEDURES AND RESULTS

Equilibrium sources of  $^{132}\text{Te}$ - $^{132}\text{I}$  and separated sources of  $^{132}\text{I}$  were used. The  $^{132}\text{Te}$  activity, which is longer lived ( $T_{1/2} = 78$  h) than  $^{132}\text{I}$  ( $T_{1/2} = 2.38$  h), has a well-known simple decay with low-energy  $\gamma$  rays, so that equilibrium sources are best for  $\gamma$ -ray studies. The  $^{132}\text{Te}$  activity for  $\gamma$ -ray studies at Vanderbilt was obtained as a fission product by neutron irradiation of an aluminum-clad ring of uranium-aluminum alloy (2.5 g of approximately 93% isotopically enriched  $^{235}\text{U}$  per 10 g Al). The irradiated ring was dissolved in caustic solution, the solutions acidified with nitric acid, and the  $^{131}\text{I}$  removed by distillation. The  $^{99}\text{Mo}$  and  $^{132}\text{Te}$  that remained in the solution were adsorbed onto an alumina column and washed with 2  $M$   $\text{HNO}_3$  and then with water. The  $^{99}\text{Mo}$  was stripped from the column

with a 1  $M$   $\text{NH}_4\text{OH}$  and with water. The  $^{132}\text{Te}$  was further purified by passing it through a Dowex 1 anion-exchange column that removed traces of  $^{99}\text{Mo}$  contamination. The  $\gamma$ -ray sources were liquid deposited onto cardboard source mounts.

For electron sources, a  $^{132}\text{I}$  generator was prepared with 60 mC of activity. To prepare the generator, the solution containing the  $^{132}\text{Te}$  activity was evaporated to dryness, taken up in 1  $M$   $\text{HNO}_3$ , diluted with water, and charged onto an alumina column (prewashed with water and with 1  $M$   $\text{HNO}_3$ ). The generator was then washed successively with water 1  $M$   $\text{NH}_4\text{OH}$ , and 0.01  $M$   $\text{NH}_4\text{OH}$ . After washing the column with the latter solution, the generator was "milked" 10–12 h later, in order to optimize the  $^{132}\text{I}/^{131}\text{I}$  ratio, by passing 10 ml of 0.01  $M$   $\text{NH}_4\text{OH}$  through the column. The 10 ml of eluate was boiled quickly in a hood, and the remaining few drops were liquid deposited on aluminum foils and covered with a Zapon film. The sources were approximately  $2 \times 22$  mm<sup>2</sup>. The backing was scratched with a sharp blade, after which insulin was used to define the source area. A typical source measured 150

<sup>14</sup> J. H. Hamilton, H. K. Carter, and J. J. Pinajian, following paper, Phys. Rev. C **1**, 666 (1970).

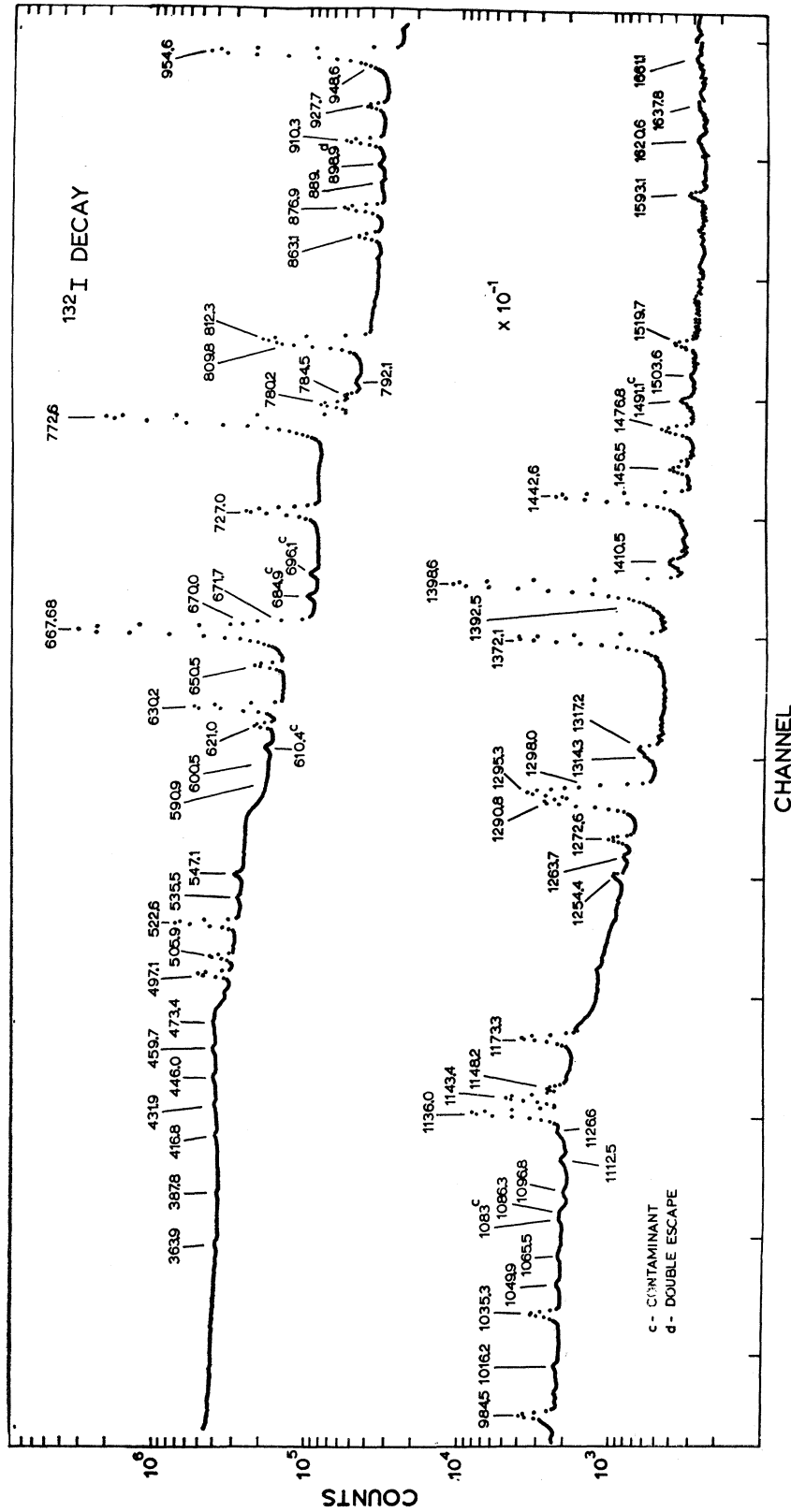


Fig. 3. Lower-energy region of the  $\gamma$ -ray singles spectra from the decay of  $^{132}\text{I}$ . These spectra were taken with a 30-cc Ge(Li) detector in conjunction with a 4096-channel analyzer. The energies of the transitions are shown.

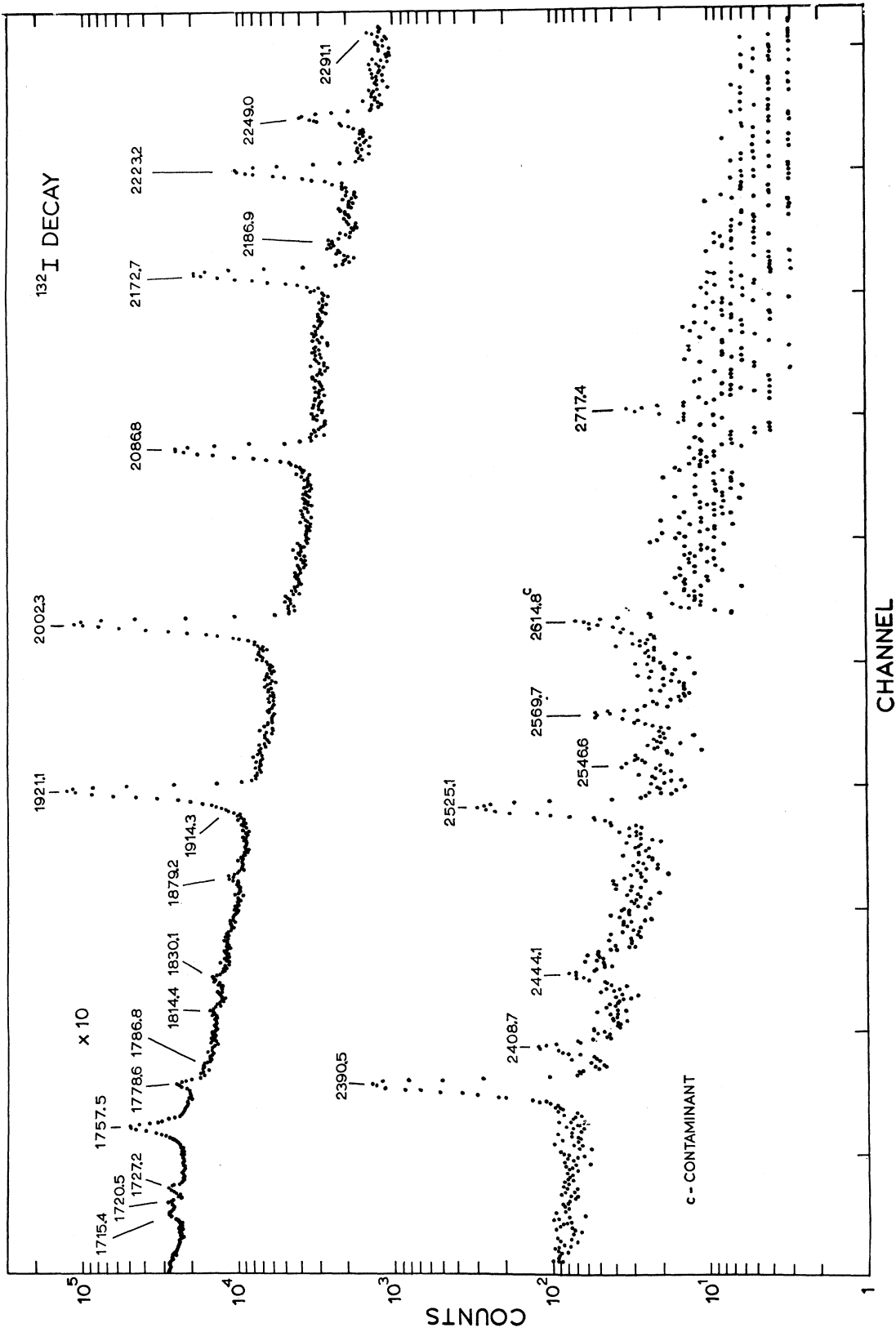
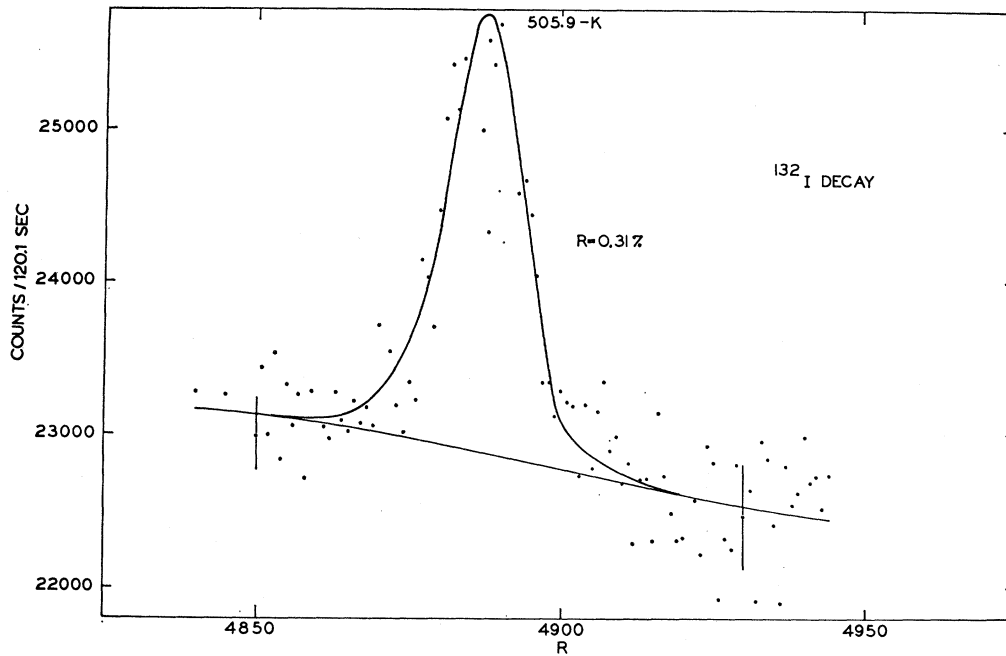
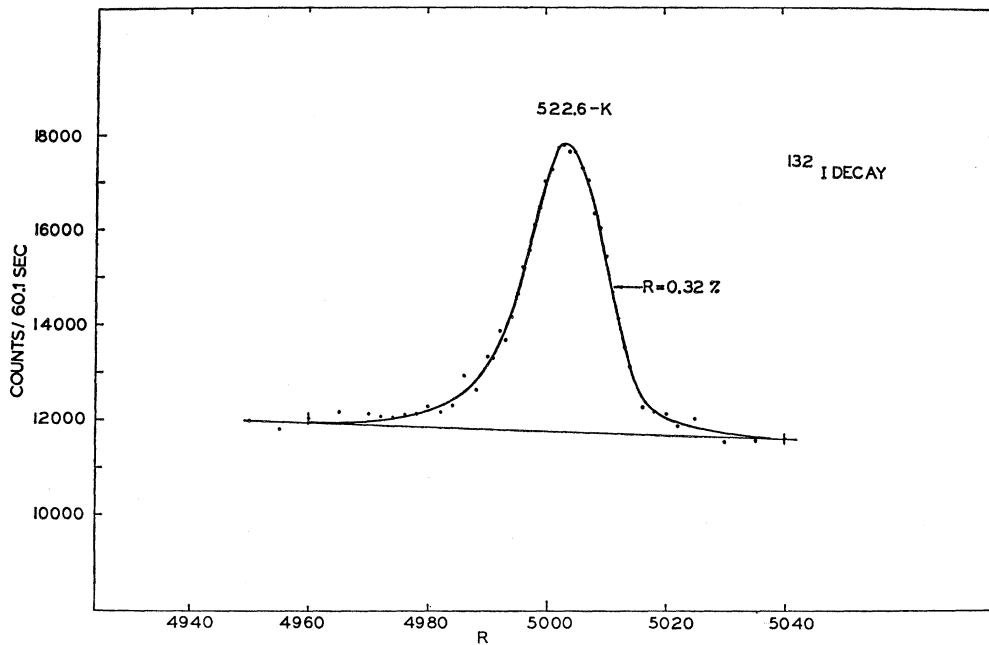


FIG. 4. High-energy region of  $\gamma$ -ray singles spectra from the decay of  $^{132}\text{I}$ . These spectra were taken with a 30-cc Ge(Li) detector in conjunction with a 4096-channel analyzer. The energies of the transitions are shown.



(a)



(b)

FIG. 5.  $K$ -conversion lines of the 505-, 727-, 522-keV transitions from the decay of  $^{132}\text{I}$ . Notice the similar resolution for all three lines, which indicates they are all essentially single lines.

millirem at 9 in. with a survey meter. No special care was taken to use thin backings or coverings, as no resolution degradation is expected at the energies studied here for reasonable coverings (less than  $1 \text{ mg/cm}^2$ ).

The  $\gamma$ -ray spectra were first measured with a  $2\text{-cm}^3$

planar Ge(Li) detector with cooled field-effect transistor and a 4096-channel Nuclear Data analyzer at Idaho Falls. The energy resolution of the spectrometer system<sup>15</sup> was 1.5-keV full width at half-maximum

<sup>15</sup> R. L. Heath, Nucl. Instr. Methods **43**, 209 (1966); USAEC Report No. IN-1300 (unpublished).

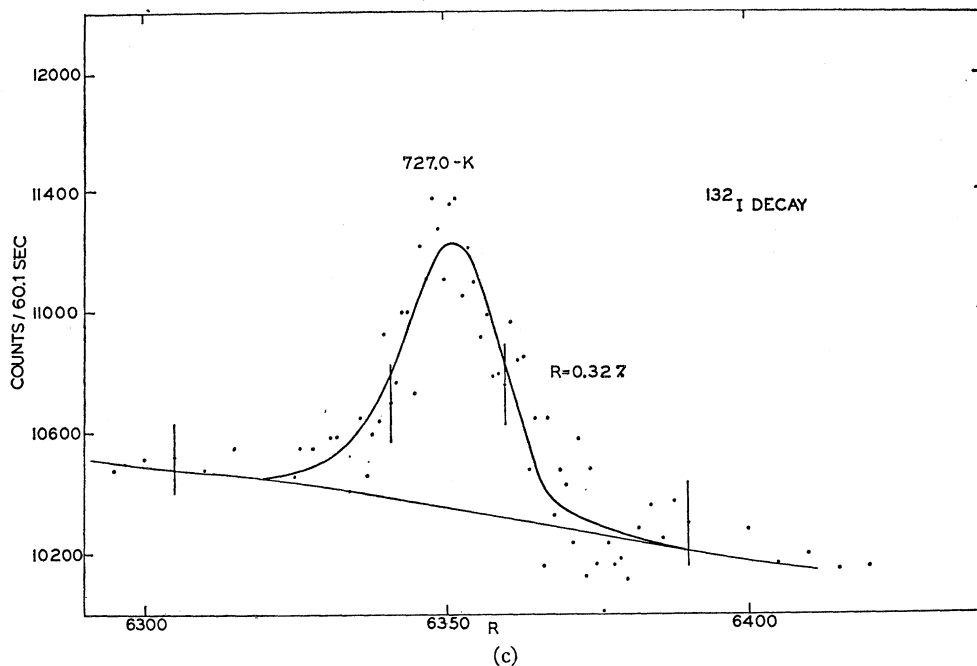


FIG. 5. (Continued).

(FWHM) at 662 keV. The sources of  $^{132}\text{Te}$  and separated  $^{132}\text{I}$  were produced by thermal-neutron irradiation at the Materials Testing Reactor. Equilibrium sources of  $^{132}\text{Te}$  ( $T_{1/2}=78$  h) and  $^{132}\text{I}$  ( $T_{1/2}=2.38$  h) and of separated  $^{132}\text{I}$  were used. Chemical procedures similar to those described above were utilized. These measurements were essential in separating some previously reported close-lying doublets and triplets at 505–507, 667–669–671, 727–729, 809–812, and 1290–1295–1298 keV. Because of the low efficiency of the detector and relatively short counting periods, many of the weak transitions were not seen. The 667–669–671-keV triplet was stripped by a computer fitting. The data were analyzed with a photopeak-analysis program.<sup>16</sup> Typical spectra of some of the doublets and triplets are shown in Figs. 1 and 2.

As good-resolution large-volume Ge(Li) detectors became available, careful studies of the  $\gamma$ -ray spectra were made with a 30-cm<sup>3</sup> trapezoidal detector with 2.1-keV FWHM system resolution at 662 keV, a Tennelec 200 amplifier and a Nuclear Data 3300 4096-channel system. This system was used for the accurate energy and intensity measurements, except for the above-mentioned doublets and triplets.

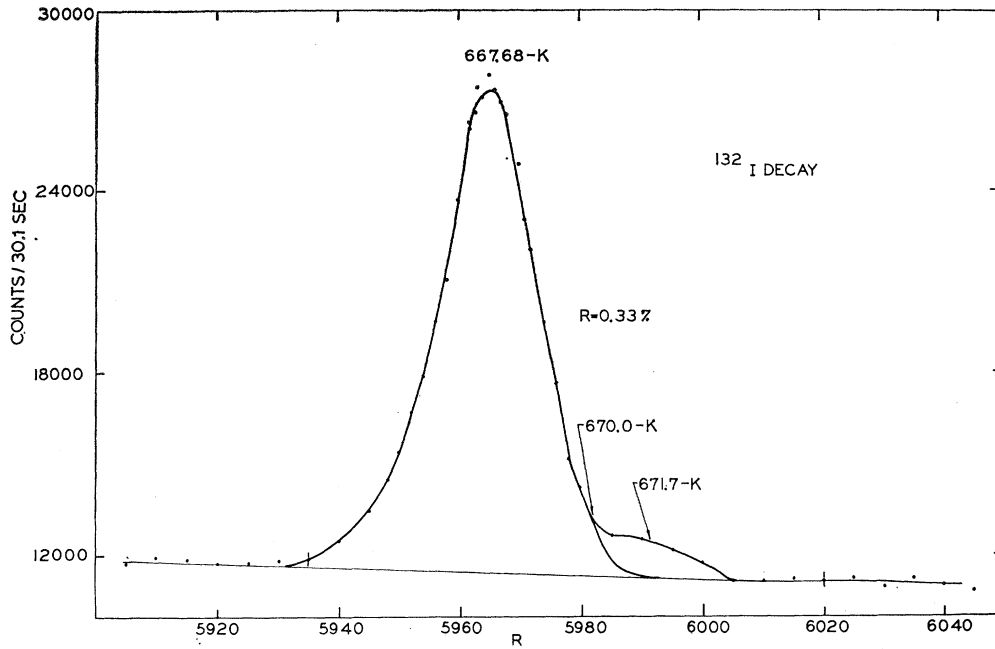
The accurate energies of the strong lines in  $^{132}\text{I}$  (identified by Ref. i in Table I) were obtained in separate measurements. In these runs, the  $^{132}\text{I}$  was mixed with various sources that contain transitions with well-known energies.<sup>17</sup> The standard sources used were

<sup>16</sup> R. G. Helmer, R. L. Heath, M. Putnam, and D. H. Gipson, Nucl. Instr. Methods **57**, 46 (1967).

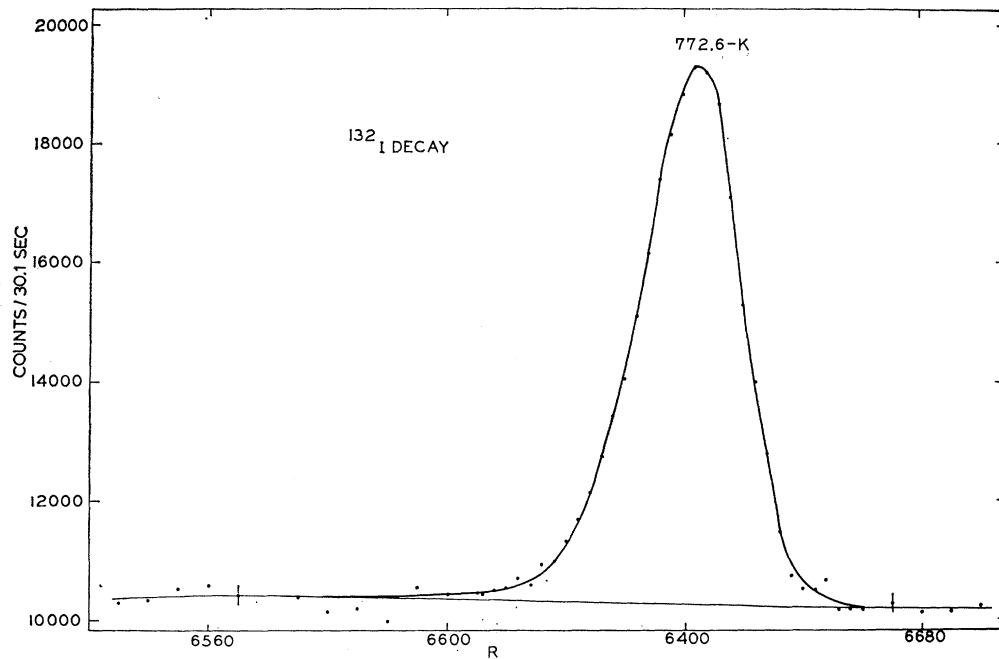
<sup>17</sup> C. M. Lederer, J. M. Hollander, and I. Perlman, in *Table of Isotopes* (John Wiley & Sons, Inc., New York, 1967).

$^{203}\text{Hg}$ ,  $^{54}\text{Mn}$ ,  $^{207}\text{Bi}$ ,  $^{22}\text{Na}$ ,  $^{137}\text{Cs}$ ,  $^{88}\text{Y}$ ,  $^{228}\text{Th}$ , and  $^{24}\text{Na}$ . In obtaining energies, the peak  $\gamma$ -ray positions were corrected for nonlinearity of the system as determined with a precision pulser and the energies versus peak positions least-squares fitted to a first-order polynomial. These results were cross-checked by a third-order-polynomial least-squares fit where no nonlinear correction was applied. These strong transitions were then used as internal calibration points in the long runs to obtain the energies of the weak transitions. In order to obtain sufficient counts in the very weak high-energy lines observed by Ythier *et al.*<sup>12</sup> without increasing the total count rate at the detector, a lead filter (9 mm) was used between the source and detector to reduce the count rate from the low-energy  $\gamma$  rays. The time for these high-energy runs was 48 h. Typical singles spectra taken with the 30-cc detector are shown in Figs. 3 and 4.

The 50-cm iron double-focusing spectrometer at Wright Patterson Air Force Base was used in the electron studies. The detector was a 5-mm $\times$ 25-mm $\times$ 3-mm-deep Si(Li) detector. It normally is operated at liquid-nitrogen temperatures; however, in these studies this was found to be impossible for the following reason. Since elemental iodine is very volatile, each time the source chamber was opened to the main chamber, the count rate began to grow and did not cease even when the source was removed. It was found that the iodine was collecting on all parts of the chamber that were cold; in particular, the iodine was deposited on the detector and its associated cold fingers. Attempts were made to improve the source covering, but no covering was found that would contain the iodine. The problem was solved when it was decided to operate the detector



(a)



(b)

Fig. 6. *K*-conversion lines of the 667- and 772-keV transitions from the decay of  $^{132}\text{I}$ .

at room temperature so that the iodine would not be preferentially deposited on the detector, and a new cold trap was placed near the source to collect any iodine that came off the source. The amount of source leakage was very small percentage wise and was of no consequence except when it collected on the detector.

With the room-temperature operation, no noticeable increase in background was observed. The only effect of operating the Si(Li) detector at room temperature was that it was necessary to raise the noise-cutoff threshold. Since the region of concern was above 500 keV, this caused no problem. The threshold which cuts



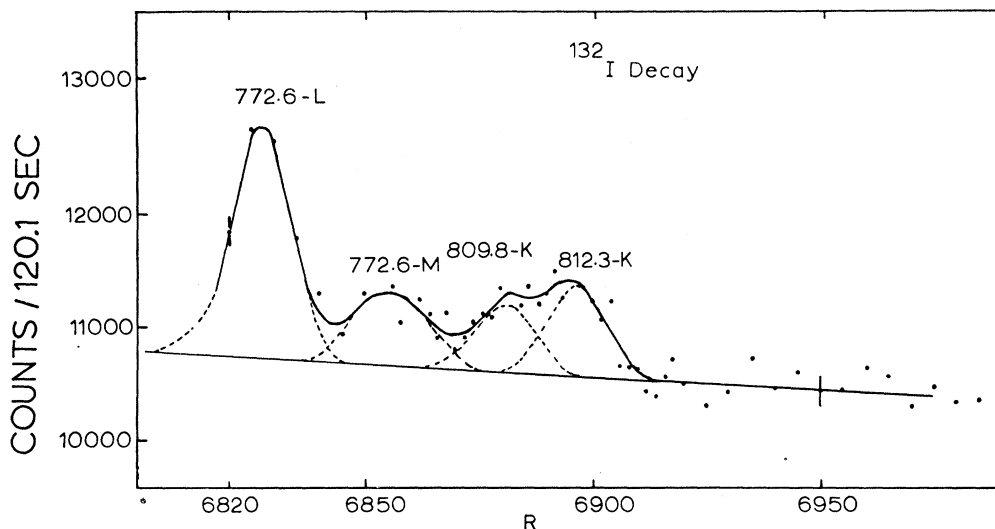


FIG. 7.  $K$ -conversion lines of the 809-, 812-keV transitions from the decay of  $^{132}\text{I}$ . The background on the left was matched up to the background at  $R=6700$  on the high-energy side of the  $K$  line of the 772.6-keV transition taken in the same run. As a test of this background, the  $K$ -line shape was fitted to the  $L$  line of the 772.6-keV transition. The background under the  $L$  line could not be significantly lowered or raised without changing the  $L$ -line intensity and subsequently the  $K/L$  ratio so as to cause disagreement with the theoretical  $K/L$  ratio. The  $K$ -line doublet of the 809- and 812.3-keV transitions was unrevealed by taking the high-energy side of the  $K$  line of the 812.3-keV transition and fitting the  $K$  line of the 772-keV transition to it. This line was subtracted and the remaining data fitted to the same  $K$ -line shape to obtain the dashed  $K$  line shown for the 809-keV transition.

out noise will also cut out different fractions, as a function of energy, of the electrons that reached the detector and backscattered out with little energy loss. By counting several standard single-conversion lines, a correction as a function of energy was obtained. This correction varied only 5% over the range of interest.

The resolution of the system was 0.30% (FWHM). Because of the short life of  $^{132}\text{I}$ , only a few lines at a time could be measured with one source. Several sources were made from successive milkings of the generator. In each run the  $K$ -conversion line of the 667- and/or the 772-keV transition was measured as a reference line, and the data were half-life corrected point by point with  $T_{1/2}=2.38$  h to the time of the start of a run. Typical spectra are seen in Figs. 5-8. The data are plotted against resistance, which is proportional to the momentum of the electrons.

The  $K$ -conversion coefficient of the 772.6-keV transition was measured by the normalized-peak-to- $\gamma$  (NPG) method where  $\alpha_K=8.94\times 10^{-2}$  for the 662-keV transition<sup>18</sup> in  $^{137}\text{Ba}$  was used as the standard. The 772.6-keV transition is a better line to use in normalizing relative electron and  $\gamma$ -ray intensities than the 667-keV one because it is not complex. The relative  $K$ -conversion lines and the  $\gamma$ -ray lines of the 772.6- and 661.6-keV transitions in  $^{132}\text{Xe}$  and  $^{137}\text{Ba}$ , respectively, were measured in the same geometries. The  $K$ -conversion coefficient of the 772.6-keV transition was found to be  $(2.73\pm 0.30)\times 10^{-3}$ , which is in agreement with the

theoretical  $E2$  value<sup>19</sup> of  $2.5\times 10^{-3}$  for this  $4^+\rightarrow 2^+$  transition.

### III. DISCUSSIONS AND CONCLUSIONS

The energies and  $\gamma$ -ray intensities of all the transitions assigned to the decay of  $^{132}\text{I}$  are presented in Table I. The results of Henck *et al.*,<sup>10</sup> Ardisson *et al.*,<sup>11</sup> Ythier *et al.*,<sup>12</sup> and Gunnink<sup>13</sup> are presented for comparison. In the data taken in this laboratory, almost all of the  $\gamma$  rays observed in the Compton-suppressed<sup>13</sup> and pair-spectrometer data<sup>12</sup> have been observed. The energies and intensities, where available, are, generally, in good agreement. The older less accurate results obtained with NaI detectors<sup>2,4,5</sup> are in good agreement with the intensities as presented in Table I and obtained with the use of Ge(Li) detectors. In this regard, one must be careful to reduce the normalization used in the NaI work and account for the composite nature of the various lines.

In Table I, it will be noted, however, that a systematic error appears to be present in one or the other of the sets of measurements in certain energy regions. The relative intensities obtained in this work and those of Henck *et al.*<sup>10</sup> are in good agreement throughout the table. There is reasonable agreement (with a few exceptions) between the two sets of measurements and the results of Ardisson *et al.*<sup>11</sup> and Ythier *et al.*<sup>12</sup> below about 1.5 MeV. However, above this energy, the latter

<sup>18</sup> J. S. Merritt and J. G. V. Taylor, *Anal. Chem.* **37**, 351 (1965).

<sup>19</sup> L. Sliv and I. M. Band, in *Alpha-, Beta-, and Gamma-Ray Spectroscopy*, edited by K. Siegbahn (North-Holland Publishing Co., Amsterdam, 1965).

TABLE I. Energies and relative intensities of  $\gamma$  rays in the decay of  $^{137}\text{I}$ . Energies are in keV.

Present work Energy	Intensity	Energy <sup>a</sup>	Energy <sup>b</sup>	Intensity <sup>b</sup>	Energy <sup>c</sup>	Intensity <sup>c</sup>	Energy <sup>d</sup>	Intensity <sup>d</sup>	Weighted average energy <sup>e</sup>	Weighted average intensity <sup>e</sup>
135.9±1.5	0.09±0.02	135	136.7±0.5	0.07±0.02					136.6±0.5	0.08±0.01
147.2±0.2	0.24±0.02	146	147.0±0.3	0.21±0.05	147.3±0.3	0.5±0.25			147.2±0.1	0.24±0.02
183.7±0.7	0.11±0.04	183	183.2±0.4	0.20±0.04					183.3±0.3	0.16±0.03
255.0±0.3	0.15±0.04	254.8	254.5±0.3	0.25±0.05					254.8±0.2	0.19±0.03
262.9±0.2	1.43±0.10	262.8	262.4±0.3	1.4±0.2	262.4±0.3	3.5±0.7			262.7±0.1	1.46±0.09
278.3±0.5	0.04±0.02 <sup>f</sup>		279.5±0.5						278.9±0.4	0.04±0.02
284.8±0.2	0.80±0.08 <sup>g</sup>	284.7	284.8±0.3	0.8±0.16	284.7±0.3	1.5±0.5			284.8±0.1	0.80±0.07
		302							302	
306.6±0.4	0.11±0.04	305.8							306.6±0.4	0.11±0.04
310.0±0.4	0.09±0.04	309.9							310.0±0.4	0.09±0.04
316.5±0.4	0.16±0.04	315.8							316.5±0.4	0.16±0.04
343.6±0.4	0.10±0.02	343.1							343.6±0.4	0.10±0.02
351.8±0.4	0.08±0.02	354.7							351.8±0.4	0.08±0.02
363.5±0.4	0.5±0.1 <sup>h</sup>	364.0							363.5±0.4	0.5±0.1
387.8±0.4	0.17±0.03	387.4							387.8±0.4	0.17±0.03
416.8±0.4	0.47±0.09	416.5							416.8±0.4	0.47±0.09
431.9±0.4	0.46±0.09	432.0							431.9±0.4	0.46±0.09
446.0±0.4	0.68±0.08	446.0							446.0±0.4	0.68±0.08
473.4±0.7	0.27±0.05								473.4±0.7	0.27±0.05
477.9±0.7	0.10±0.04	478							477.9±0.7	0.10±0.04
487.5±0.7	0.18±0.05 <sup>i</sup>	488.0							487.5±0.7	0.18±0.05
505.94±0.15 <sup>i</sup>	5.0±0.2	506.0	505.8±0.3	5.1±0.8	505.8±0.5	5.4±0.5			505.90±0.13	5.1±0.2
522.04±0.10 <sup>i</sup>	16.5±0.8	522.8	522.7±0.3	15.5±1	522.7±0.4	18.3±2			522.65±0.09	16.3±0.6
535.5±0.4	0.53±0.08	535.5							535.5±0.4	0.53±0.08
547.1±0.3	1.15±0.10	546.9	547.4±0.4		546.4±0.6	2.4±0.3			547.1±0.2	1.27±0.09
590.9±2.0	0.06±0.04	591							590.9±2.0	0.06±0.04
600.5±2.0	0.09±0.03	599.7							600.5±2.0	0.09±0.03
621.0±0.2	2.0±0.10	621.0	620.8±0.4	1.9±0.3	621.7±0.5	1.8±0.4			621.0±0.2	2.0±0.1
630.21±0.10 <sup>i</sup>	14.1±0.7	630.3	630.2±0.3	13.5±1.3	630.4±0.5	13.1±2			630.22±0.09	13.9±0.6
636.8	<sup>137</sup> I	636.8								
650.5±0.2	2.5±0.2	650.6	650.8±0.3	3±0.5	651.0±0.5	6.7±1.1			650.6±0.2	2.7±0.2
		659.0	652.1						659.0	
667.68±0.08 <sup>i</sup>	100	667.7	667.8±0.3	100	667.8±0.5	100			667.69±0.08	100
670.0±0.4	4.4±0.8	670.7	669.6±0.4	10.7±2.5					669.8±0.3	5.0±0.8
671.7±0.4	6.1±0.6	675	671.4±0.4	4.4±0.6					671.6±0.3	5.3±0.4
727.0±0.2	6.6±0.4	727.3	727.4±0.3	5.7±0.9	727.3±0.6	7.6±0.8			727.1±0.2	6.6±0.3
729.2		729.5±0.4	729.5±0.4	1.1±0.3						

TABLE I. (Continued).

Present work		Energy <sup>a</sup>	Intensity <sup>b</sup>	Energy <sup>b</sup>	Intensity <sup>b</sup>	Energy <sup>c</sup>	Intensity <sup>c</sup>	Energy <sup>d</sup>	Intensity <sup>d</sup>	Weighted average energy <sup>e</sup>	Weighted average intensity <sup>e</sup>
Energy	Intensity										
772.60±0.08 <sup>i</sup>	76.5±2.0	764.5		772.8±0.3	79±5	772.6±0.6	86.6±9			764.5	
780.2±0.4	1.25±0.06	772.7		780.2±0.4						772.61±0.08	77.2±1.8
784.5±0.4	0.43±0.05	780.0								780.2±0.3	1.25±0.06
792.1±1.0	0.09±0.03	784.5								784.5±0.4	0.43±0.05
809.8±0.3	2.7±0.3	791.4		809.7±0.4	4.3±0.8					792.1±1.0	0.09±0.03
812.3±0.3	5.7±0.6	810		812.3±0.4	5.8±1.2	811.3±0.6	9.8±1			809.8±0.2	2.9±0.3
		812.3		861.7±0.5						812.2±0.2	5.7±0.5
863.1±0.2	0.59±0.05	863.2		864.4±0.5	0.5±0.2	863.9±0.6	0.9±0.2			861.7±0.5	
876.9±0.3	1.10±0.05	877.0		876.6±0.4	1±0.2	877.0±0.8	1.1±0.2			863.3±0.2	0.60±0.05
889.0±2	0.04±0.03	889.1								876.8±0.2	1.09±0.05
910.3±0.2	0.93±0.05	910.3		910.2±0.4	1.9±0.5	910.8±0.8	0.8±0.2			889.0±2	0.04±0.03
927.7±0.3	0.41±0.08	927.7		927.3±0.5	1.0±0.3					910.3±0.2	0.93±0.05
948.6±2	0.08±0.05	947.1								927.6±0.3	0.45±0.08
954.55±0.10 <sup>i</sup>	18.0±0.9	954.6		954.5±0.3	18±1	954.9±0.7	21.3±2.0			948.6±2	0.08±0.05
984.5±0.3	0.73±0.07	984.4		984.4±0.5		985.2±1.0	0.25±0.10			954.55±0.09	18.3±0.6
		1002.1								984.5±0.2	0.57±0.06
		1009.8								1002.1	
1016.2±2.0	0.05±0.03	1009.8								1009.8	
1035.3±0.3	0.57±0.05	1035.4		1034.1±0.3	0.6±0.2	1035.0±1.0	0.70±0.20			1016.2±2.0	0.05±0.03
1049.9±0.7	0.045±0.015	1050.2								1034.7±0.2	0.58±0.05
1065.5±0.7	0.034±0.011	1065.5±0.7								1049.9±0.7	0.045±0.015
1086.3±1.0	0.070±0.030	1087.0								1065.5±0.7	0.034±0.011
1096.8±0.7	0.035±0.012	1097.0								1086.3±1.0	0.070±0.030
1112.5±0.4	0.063±0.021	1113.3								1096.8±0.7	0.035±0.012
1126.6±0.7	0.052±0.024	1126.6								1112.5±0.4	0.063±0.021
1136.03±0.12 <sup>i</sup>	2.9±0.2	1136.0		1136.0±0.5	4±0.6	1135.7±1.2	3.0±0.6			1126.6±0.7	0.052±0.024
1138	≤0.3	1138								1136.03±0.12	3.0±0.2
1143.4±0.2 <sup>i</sup>	1.4±0.1	1143.6		1143.7±0.5	1.4±0.4	1143.5±1.5	2.0±0.6			1138	≤0.3
1148.2±0.7	0.21±0.05	1148								1143.4±0.2	1.4±0.1
1173.3±0.2	1.1±0.1	1173.2		1172.9±0.5	1.1±0.3	1171.0±1.5	0.7±0.3			1148.2±0.7	0.21±0.05
1254.4±0.7	0.046±0.023	1254.0		1253.6±0.8						1173.2±0.2	1.1±0.1
1263.7±0.7	0.023±0.012	1263.7								1254.1±0.5	0.046±0.023
1272.6±0.4	0.15±0.03	1272.5		1273.3±0.8						1263.7±0.7	0.023±0.012
1290.8±0.4	1.12±0.06	1290.8		1290.5±0.6	1.5±0.2					1272.7±0.4	0.15±0.03
1295.3±0.4	1.8±0.2	1295.5		1296.0±0.6	1.7±0.2	1293.9±1.5	2.2±0.3	1294.2±1.0	2.3±0.3	1290.7±0.3	1.15±0.06
1298.0±0.6	0.78±0.08	1298.0				1299.0±1.5	1.7±0.2	1298.4±1.5	1.1±0.3	1295.3±0.3	2.0±0.1
1314.3±0.7	0.060±0.020	1314.2								1298.2±0.5	0.9±0.1
1317.2±0.7	0.090±0.030	1317.7		1316±2	0.16±0.04					1314.3±0.7	0.060±0.020
										1317.1±0.7	0.12±0.02

TABLE I. (Continued).

Present work		Present work				Present work				Present work	
Energy	Intensity	Energy <sup>a</sup>	Intensity <sup>b</sup>	Energy <sup>b</sup>	Intensity <sup>b</sup>	Energy <sup>c</sup>	Intensity <sup>c</sup>	Energy <sup>d</sup>	Intensity <sup>d</sup>	Weighted average energy <sup>e</sup>	Weighted average intensity <sup>e</sup>
1372.10±0.14	2.3±0.2	1372.0		1324.0±0.6		1371.5±1.2	2.9±0.3	1372.2±1.2	2.5±0.3	1324.0±0.6	2.5±0.1
1392.5±2.0	0.24±0.15	1390.7		1371.8±0.5	2.6±0.4					1372.07±0.13	0.24±0.15
1398.57±0.10 <sup>i</sup>	6.9±0.4	1398.5		1398.4±0.5	7.3±0.8	1398.4±1.2	7.6±0.8	1399.5±1.2	7.6±0.8	1392.5±2.0	7.2±0.3
1410.5±0.4	0.06±0.02	1411.1								1398.57±0.10	0.06±0.02
1442.56±0.10 <sup>i</sup>	1.43±0.08	1442.5		1442.5±0.5	1.4±0.2	1442.5±1.2	1.5±0.2	1443.0±1.2	1.44±0.15	1442.56±0.10	1.44±0.06
1456.5±0.2	0.049±0.010	1456.6								1456.5±0.2	0.049±0.010
1476.8±0.2	0.13±0.02	1476.5		1476.4±0.8				1479.0±1.5	0.18±0.05	1476.8±0.2	0.14±0.02
1503.6±0.6	0.009±0.003									1503.6±0.6	0.009±0.003
1519.7±0.2	0.075±0.008	1519.0		1519.7±0.8				1520.0±2.0	0.018±0.01	1519.7±0.2	0.052±0.006
1542.2±1.0	0.010±0.005	1544.7								1542.2±1.0	0.010±0.005
1593.1±0.3	0.045±0.006	1592						1593.6±2.0	0.07±0.03	1593.1±0.3	0.045±0.006
1620.6±0.7	0.030±0.006	1619								1620.6±0.7	0.030±0.006
1637.8±0.7	0.017±0.004	1640 <sup>j</sup>								1637.8±0.7	0.017±0.004
1661.6±0.7	0.017±0.004	1673 <sup>i</sup>								1661.6±0.7	0.017±0.004
1715.4±0.6	0.053±0.005	1715 <sup>i</sup>		1715.8±1.0						1715.5±0.5	0.053±0.005
1720.5±0.6	0.048±0.005	1720 <sup>j</sup>		1723±3		1722.0±2.5	0.10±0.03	1722.2±2.0	0.14±0.02	1720.5±0.6	0.056±0.005
1727.2±0.6	0.063±0.009	1727 <sup>i</sup>		1727.5±1.0	0.13±0.03					1727.3±0.5	0.063±0.009
1738.0	<0.018			1738.0±1.0						1738.0	<0.018
1747.0	<0.018			1747.0±1.0						1747.0	<0.018
1757.5±0.2 <sup>i</sup>	0.34±0.04	1757		1756.0±0.8	0.45±0.05	1756.2±3.0	0.4±0.1	1758.2±1.5	0.44±0.05	1757.5±0.2	0.38±0.03
1778.6±0.7	0.060±0.015	1777		1778.0±0.8				1778.9±2.5	0.094±0.020	1778.6±0.7	0.060±0.015
1786.8±1.0	0.008±0.004	1784 <sup>i</sup>								1786.8±1.0	0.008±0.004
1803	<0.002									1803	<0.002
1814.4±0.7	0.010±0.004	1811 <sup>i</sup>		1828±3	0.06±0.02					1814.4±0.7	0.010±0.004
1830.1±0.7	0.022±0.010	1827 <sup>i</sup>								1830.0±0.7	0.029±0.009
1879.2±0.7	0.016±0.003									1879.2±0.7	0.016±0.003
1914.3±0.7	0.06±0.05	1913 <sup>i</sup>								1914.3±0.7	0.06±0.05
1921.08±0.12 <sup>i</sup>	1.2±0.1	1921		1920.7±0.6	1.3±0.2	1921.2±2.0	1.44±0.15	1922.2±1.5	1.52±0.15	1921.08±0.12	1.2±0.09
1985.5±1.5	0.008±0.002									1985.5±1.5	0.008±0.002
2002.3±0.12 <sup>i</sup>	1.1±0.1	2003		2002.1±0.6	1.1±0.2	2002.3±2.0	1.41±0.20	2002.9±1.5	1.70±0.17	2002.30±0.12	1.1±0.1
2086.84±0.15 <sup>i</sup>	0.23±0.05	2088		2086.1±0.8	0.27±0.06	2087.7±2.0	0.32±0.06	2086.9±1.5	0.39±0.04	2086.82±0.15	0.25±0.04
2172.67±0.15 <sup>i</sup>	0.20±0.04	2175		2173.1±0.8	0.18±0.05	2173.5±2.5	0.31±0.06	2172.2±1.5	0.38±0.04	2172.68±0.15	0.19±0.03
2186.9±2.0	0.007±0.003									2186.9±2.0	0.007±0.003
2204	<0.002			2204.1±1.0						2204.1	<0.002
2223.15±0.15 <sup>i</sup>	0.12±0.02	2226		2223.6±0.8	0.12±0.04	2224.6±2.5	0.21±0.04	2223.7±1.7	0.21±0.03	2223.17±0.15	0.12±0.02
2249.0±0.4	0.03±0.01	2252		2249.3±0.8	0.03±0.01	2250.6±2.5	0.07±0.02	2248.7±2.0	0.06±0.01	2249.1±0.3	0.03±0.01
2291.1±1.5	0.004±0.002			2286	0.03±0.01			2288.5±2.5	0.011±0.005	2290.4±1.3	0.017±0.005

TABLE I. (Continued).

Present work		Present work		Present work		Present work		Present work		Present work		Present work		
Energy	Intensity	Energy <sup>a</sup>	Energy <sup>b</sup>	Intensity <sup>b</sup>	Energy <sup>c</sup>	Intensity <sup>c</sup>	Energy <sup>d</sup>	Intensity <sup>d</sup>	Weighted average energy <sup>e</sup>	Weighted average intensity <sup>e</sup>	Energy <sup>f</sup>	Intensity <sup>f</sup>	Weighted average energy <sup>g</sup>	Weighted average intensity <sup>g</sup>
2390.48±0.15 <sup>i</sup>	0.17±0.03	2395	2390.9±0.8	0.18±0.03	2392.3±2.5	0.30±0.06	2391.1±1.5	0.32±0.03	2390.48±0.15	0.17±0.02			2390.48±0.15	0.17±0.02
2408.7±0.7	0.010±0.003		2408.8±1.0				2412.2±2.5	0.014±0.010	2408.9±0.6	0.010±0.003			2408.9±0.6	0.010±0.003
2444.1±0.7	0.004±0.002		2449.8±1.0	0.006±0.002			2447.3±2.5	0.012±0.004	2446.04±0.6	0.005±0.002			2446.04±0.6	0.005±0.002
2454.6±0.7	0.003±0.002		2456.4±1.0				2454.6±3.0	0.009±0.005	2455.2±0.6	0.003±0.002			2455.2±0.6	0.003±0.002
2487.6	<0.002						2486.0±3.0	0.008±0.005	2487	<0.002			2487	<0.002
2525.12±0.15 <sup>i</sup>	0.036±0.009	2526	2525.7±1.0	0.04±0.01	2525.9±2.5	0.08±0.02	2525.5±1.8	0.080±0.008	2525.14±0.15	0.037±0.007			2525.14±0.15	0.037±0.007
2546.6±1.5	0.002±0.001						2568.0±2.5	0.012±0.004	2546.6±1.5	0.002±0.001			2546.6±1.5	0.002±0.001
2569.7±0.7	0.003±0.001		2569.9±1.0	0.003±0.001	2569.1±4.0	0.01±0.002	2591.0±3.0	0.005±0.003	2569.7±0.6	0.003±0.001			2569.7±0.6	0.003±0.001
2591.0	<0.0005						2605.0±4.0	<0.005	2591.0	<0.0005			2591.0	<0.0005
2605.0	<0.0005						2615.3±3.0	0.003±0.002	2605.0	<0.0005			2605.0	<0.0005
2614.8±0.7	<0.006		2618.3±1.0		2611.6±5.0	0.002±0.001	2655.3±3.0	0.007±0.002	2614.8±0.7	<0.006			2614.8±0.7	<0.006
2652.1	<0.0005		2660±4	0.001±0.0005			2689.9±3.0	0.004±0.001	2689.9	<0.0005			2689.9	<0.0005
2689.9	<0.0005						2717.8±3.0	0.009±0.005	2717.4±0.7	0.003±0.001			2717.4±0.7	0.003±0.001
2717.4±0.7	0.003±0.001				2717.0±5.0	0.010±0.005	2764.2±4.0	<0.005	2764.2	<0.001			2764.2	<0.001
2764.2	<0.001						2838.6±4.0	<0.004	2838.6	<0.004			2838.6	<0.004

<sup>a</sup> Reference 13.<sup>b</sup> Henck *et al.*, Refs. 8 and 10.<sup>c</sup> Ardisson *et al.*, Ref. 11.<sup>d</sup> Ythier *et al.*, Ref. 12.<sup>e</sup> The energies of Ref. 13 were not used in the averages. The intensities above 1.5 MeV of Refs. 11 and 12 were not used in the averages.<sup>f</sup> Intensity of this line in  $^{132}\text{I}$  decay deduced from the relative intensities (Ref. 17) in the  $^{132}\text{Te}$  decay. The maximum intensity of the 459.7-keV transition in  $^{132}\text{Te}$  was determined to be 0.55 relative to the<sup>g</sup> Transitions seen in spectra of Ref. 13 but not reported by them.667.7-keV transition of  $^{132}\text{I}$ .<sup>h</sup> A transition of this energy appears in  $^{132}\text{I}$ . The intensity of this line in the  $^{132}\text{I}$  decay was determined from the intensity of the 363-keV line in the  $^{132}\text{I}$  decay and the  $^{132}\text{I}$  relative intensities.<sup>i</sup> A transition of this energy appears in  $^{132}\text{I}$ . The intensity of this line in the  $^{132}\text{I}$  decay was deduced from the relative intensities of the 363- and 505-keV transitions as determined from the  $^{132}\text{Cs}$  decay.<sup>j</sup> The energy of this transition was measured in separate runs with calibration standards mixed with the source.

TABLE II. *K*-conversion coefficients in the decay of  $^{132}\text{I}$ . The electron intensities were taken from the last column of Table III and  $\gamma$ -ray intensities from the last column of Table I.

Trans. energy (keV)	Experimental $\alpha_K(10^{-3})$	Theoretical $\alpha_K(10^{-3})^a$			Multipolarity assignment
		<i>E1</i>	<i>M1</i>	<i>E2</i>	
136.6	306±137	76	290	450	<i>M1-E2</i>
147.2	135±34	62	240	360	
183.3	127±41	35	138	175	<i>M1-E2</i>
254.8	77±23	13.5	56	57	<i>M1-E2</i>
262.7	44±7	12.8	54	55	<i>M1-E2</i>
284.7	31±7	10.2	40	41	<i>M1-E2</i>
505.9	6.2±1.5	2.45	9.7	7.4	( <i>E2</i> )
522.6	7.9±0.8	2.25	8.8	6.8	<i>M1-E2</i>
621.0	8.8±2.5	1.55	5.6	4.3	<i>M1-E2</i>
630.2	4.2±0.5	1.50	5.5	4.1	<i>M1-E2</i>
650.6	6.5±2.7	1.40	5.1	3.8	( <i>M1-E2</i> )
667.7	3.5±0.3	1.32	4.8	3.6	<i>E2</i>
669.8	4.9±1.6	1.32	4.8	3.6	<i>M1-E2</i>
671.5	4.0±1.4	1.32	4.8	3.6	<i>M1-E2</i>
727.1	2.7±0.6	1.14	4.0	2.90	( <i>M1</i> ) <i>E2</i>
772.6	2.73±0.30 <sup>b</sup>	1.00	3.4	2.55	<i>E2</i>
809.8	2.9±0.6	0.90	3.0	2.25	<i>M1-E2</i>
812.3	2.2±0.4	0.90	3.0	2.25	<i>M1-E2</i>
954.6	1.99±0.24	0.66	2.1	1.56	<i>M1-E2</i>
1136.0	1.51±0.29	0.47	1.38	1.05	<i>M1-E2</i>
1143.4	2.05±0.45	0.46	1.38	1.04	<i>M1-(E2)</i>
1173.2	1.24±0.36	0.45	1.28	0.94	<i>M1-E2</i>
1372.1	0.98±0.21	0.34	0.87	0.72	<i>M1-E2</i>
1398.6	0.93±0.13	0.33	0.84	0.70	<i>M1-E2</i>
1439.4 <sup>c</sup>	>300				<i>E0</i>

<sup>a</sup> Reference 19.<sup>b</sup> Normalization line.<sup>c</sup> Not in  $^{132}\text{I}$ .

two groups's values are often twice the values obtained in this work and in the work of Henck *et al.* Thus, it appears that a systematic error is introduced in one of the pairs of measurements. The only apparent source for such an error is the determination of the efficiency curve. In the present measurements, the shape of the efficiency curve was checked in the range of 1300-2700 keV by calculating the relative intensities of  $^{24}\text{Na}$  from the efficiency curve determined by  $^{56}\text{Co}$ . The results were within 2% of the accepted values.<sup>20</sup> Similar results were obtained when the efficiency curve was applied to the 583- and 2614-keV lines of  $^{228}\text{Th}$ . Thus, it is thought that systematic errors in the present intensity measurements are less than 2%. Therefore, the intensities of Ardisson *et al.*<sup>11</sup> and Ythier *et al.*<sup>12</sup> were not used in the averages beyond 1660 keV. The impurities that were identified and the intensities of the strongest transitions in these decays relative to 667-keV transition of  $^{132}\text{I}$  (as being 100) were as follows:  $^{131}\text{Te}$  (854 keV, 0.09),  $^{129}\text{Te}$  (460 keV, 0.55), and  $^{103}\text{Ru}$  (497 keV, 8.0).

One notes that the doublets at 505, 727<sup>3</sup> and 650<sup>1</sup> keV were not found in this work. Figure 2 shows two

different spectra of the 727-keV region taken at 1.5 keV resolution (FWHM). These spectra, which were taken with different sources ( $^{132}\text{Te}$ - $^{132}\text{I}$  and separated  $^{132}\text{I}$ ), show that the 729-keV  $\gamma$  ray is a contaminant in  $^{132}\text{I}$ . The evidence against transitions at 507 and 652 keV is not as conclusive. However, transitions of the energy and intensity reported earlier<sup>1,3</sup> were not observed in these measurements. Most of the intensities reported earlier for these transitions were probably from impurities. Another interesting point is that the intensity of the transition at 650 keV is approximately one-half the intensity observed for this transition by Ardisson *et al.*,<sup>11</sup> so that the impurity member of the doublet may be showing up in their measurements. The conversion-electron intensities obtained in this and other work<sup>1-3,9</sup> are given in Table II.

The conversion-electron measurements confirm that the 505.9- and 727.0-keV transitions are in fact single lines, as seen in Fig. 5. These data confirm the  $\gamma$ -ray measurements on this point. It is quite possible that the *K* intensity of the 505.9-keV transition is underestimated in the work of Boyd and Hamilton,<sup>3</sup> who divided the intensity between two transitions at this energy. Thus, this intensity was not used in averages. A closer

<sup>20</sup> J. B. Marion, Nucl. Data 4, 308 (1968), Sec. A.

TABLE III. Intensities of  $K$ -conversion electrons in the decay of  $^{132}\text{I}$ .

Trans. energy (keV)	Present work	a	b	c	d	Weighted averages <sup>e</sup> $I_e$
136.6		7±3				7±3
147.2		11.5±2.5		9±2	7.5±1.7	9.3±2
183.3		5.8±1.5				5.8±1.5
254.8		4.2±1.0				4.2±1
262.7		17.5±2.0	19±3		15.5±2	17.5±2
284.7		8.3±1.2			5.7±2.0 <sup>f</sup>	7.0±1.1
505.9	10.8±1.5		5±2		5.2±2.4 <sup>f</sup>	9±1.2
507	...		6.6±2			
522.6	43.5±3.7		37±2		33±3	36.7±1.5
621.0		5.6±2		4±2	5.8±3	5.0±1.3
630.2			18±2	16±2	16.5±2	16.8±1.2
650.6			6±2	4±2		5±2
652				4±2		
667.7		100 <sup>g</sup>	100 <sup>g</sup>	100 <sup>g</sup>	118 <sup>g</sup>	100 <sup>g</sup>
669.8	113 <sup>g</sup>			7±2		7±2
671.5				6±2		6±2
727.1	5.6±1.5		4±1.5		5.2±1.2	5.0±1.0
729	...		4±1.5			
772.6	57±3	61±2	57±4	61±2	73±6	60.2±1.5
772.6L	8.6±1.9					
772.6M+...	3.9±0.8				12.7	
809.8	2.7±0.6	2.0±0.5				2.4±0.4
812.3	3.9±0.5	3.2±0.5				3.6±0.4
954.6	10.5±1.0		10±2	9.7±1.5	12.6±3	10.4±0.7
1136	1.4±0.3		1.0±0.3			1.3±0.2
1143.4	0.82±0.16		0.5			0.82±0.16
1173.2	0.39±0.10					0.39±0.10
1372.1	0.70±0.14					0.70±0.14
1398.6	1.92±0.22		2.0±0.5		2±2	1.93±0.20
1439	3.4±0.7					3.4±0.7 <sup>h</sup>

<sup>a</sup> Henck, Ref. 8.<sup>b</sup> Boyd and Hamilton, Ref. 3.<sup>c</sup> Hamilton *et al.*, Ref. 1.<sup>d</sup> Johnson *et al.*, Ref. 2.<sup>e</sup> The 505.9-keV transition of Boyd and Hamilton was not used in averaging the data.

ing the data.

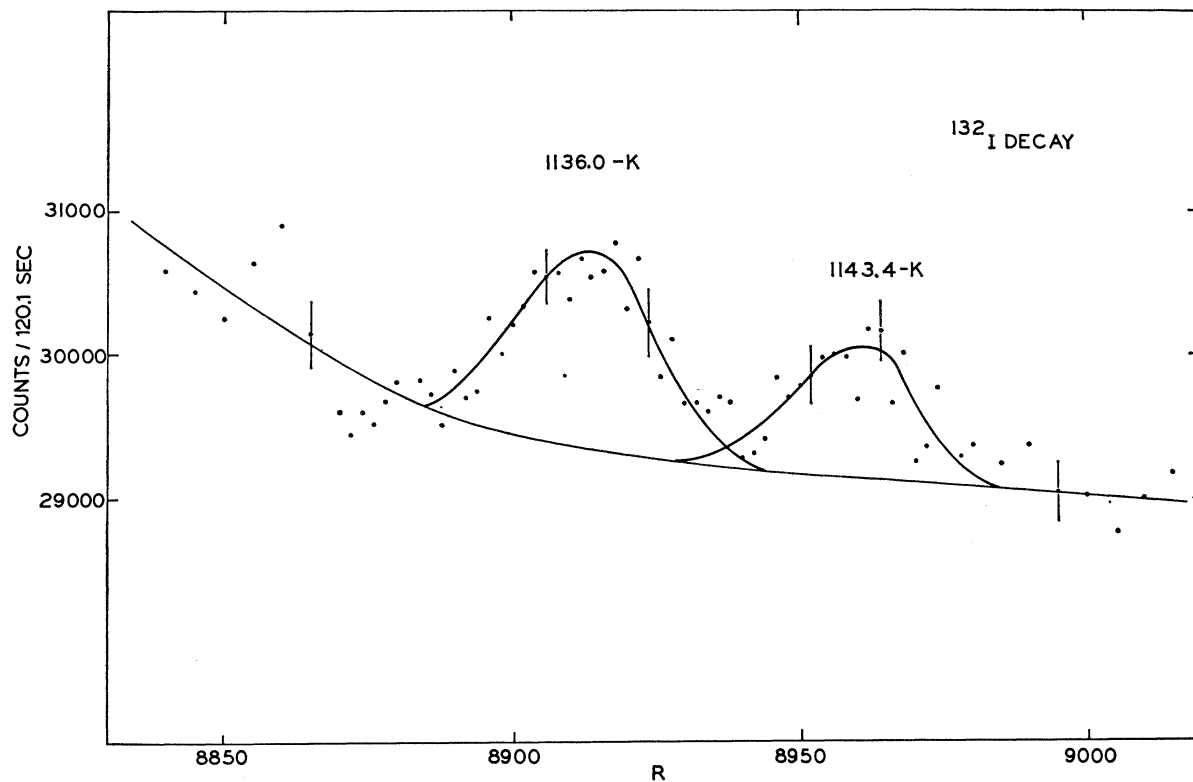
<sup>f</sup> Reference 21.<sup>g</sup> Normalization line.<sup>h</sup> Not in  $^{132}\text{Xe}$ .

look<sup>21</sup> at the data of Johnson *et al.*<sup>2</sup> indicated that the  $K$  intensities of the 505.9- and 284.7-keV transitions should be increased.

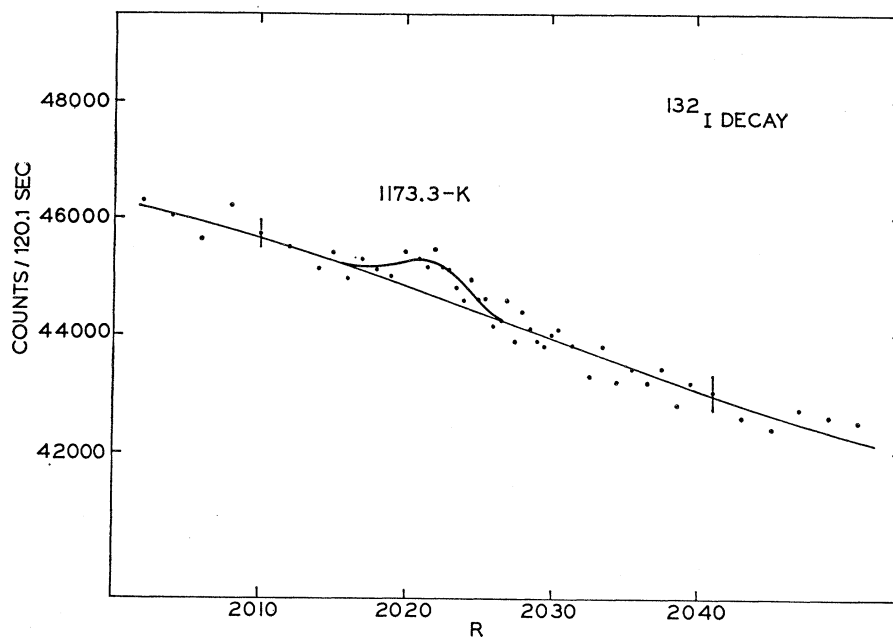
There was considerable disagreement in the 809–812-keV intensities between the present results and those first reported by private communication from Henck.<sup>8</sup> However, the value obtained for the  $K:L:(M+\dots)$  ratio of the 772.6-keV transition in the same run (Fig. 3) is in good agreement with an earlier measurement by Johnson *et al.*<sup>2</sup> and is also in reasonable agreement with theory. The background in Fig. 3 was made to match up with the background on the low-energy side of the  $K$  line of the 772.6-keV transition. Their results for the 809- and 812-keV electron intensities were rechecked, and their results<sup>8</sup> submitted for publication are now in agreement with our results.

<sup>21</sup> N. R. Johnson (private communication).

The conversion coefficients are shown in Table II. It will be noted that with more  $\gamma$ -ray intensities made available by the present high-resolution  $\gamma$ -ray experiments and with additional conversion-electron intensities made available by this work and the work of Henck,<sup>8</sup> there are 21 more conversion coefficients known now than were known at the time of the paper of Hamilton *et al.*<sup>6</sup> There are several points worth noting. First, a multipolarity assignment for the 1143.4-keV transition can now be made. It is well established that both the electron and  $\gamma$ -ray intensity of the 1143.4-keV transition are approximately one-half of the 1136.0-keV transition. The electron data of Boyd and Hamilton<sup>3</sup> are consistent with this in that a transition of one-half the intensity of the 1136-keV one cannot be ruled out, but the earlier rough  $\gamma$ -ray data<sup>4</sup> are not consistent. Therefore, the conversion coefficients of both



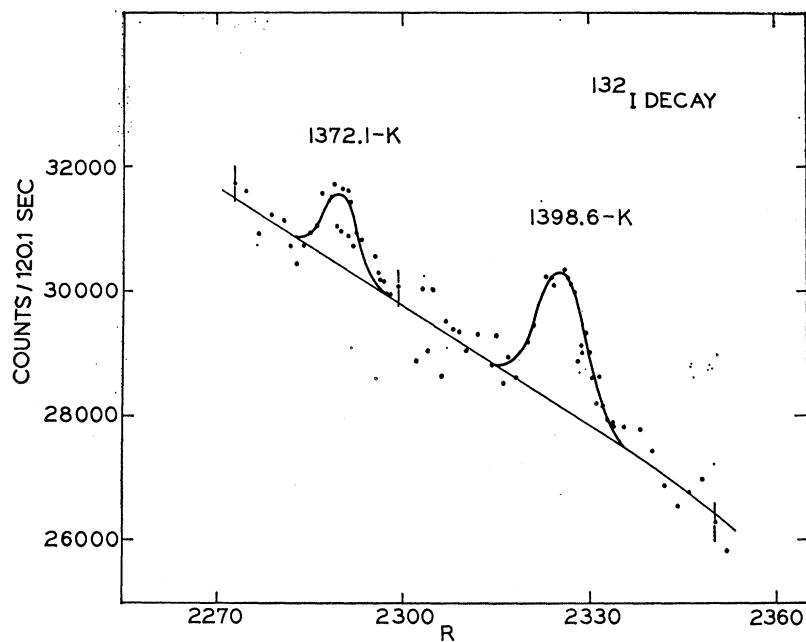
(a)



(b)

FIG. 8. The K-conversion lines of the 1136-, 1143-, 1173-, 1372-, and 1398-keV transitions from the decay of  $^{132}\text{I}$ .





(c)

FIG. 8. (Continued).

transitions are in reasonable agreement with  $M1$  and/or  $E2$ .

From the tentative  $E1$  assignment of the 1143.4-keV transition,<sup>3</sup> Hamilton *et al.*<sup>6</sup> also assigned the 621.0-keV transition from the same level as the 1143-keV one to be  $E1$  in their decay scheme. From Table III, one sees that the conversion-electron intensities of the 621.0-keV transition obtained by Hamilton *et al.*<sup>1</sup> and that of Henck<sup>8</sup> and Johnson *et al.*<sup>2</sup> are in agreement. Also, the relative  $\gamma$ -ray intensities for the 621.0-keV transition are in good agreement. From these data, the conversion coefficient of this transition is well established as  $M1$  or  $E2$ , not  $E1$ .

A point of interest is the observation of a transition at 1439.4 keV with a large  $K$ -electron intensity more characteristic of an  $E0$  transition. Unfortunately, only one run was taken in this energy range, so the assignment of this peak to  $^{132}\text{I}$  could not be substantiated. Also, the resolution of the 1439-keV line is larger (0.6%) than that of the 772.6-keV line (0.35%) taken in the same run. The poor resolution could arise in part from the  $K$  line of the 1442-keV transition. In very recent work, only the 1442-keV transition was ob-

served.<sup>22</sup> Thus, the 1439-keV transition is not in  $^{132}\text{Xe}$ .

With the establishment of all transitions for which electron data are available as  $M1$  and/or  $E2$ , there is no evidence for any odd-parity levels populated in  $^{132}\text{Xe}$  by  $^{132}\text{I}$ . It is possible, however, that some of the weakly populated levels could be odd-parity  $3^-$  states. This possibility is considered by Carter *et al.*<sup>22</sup> The implications of these data in assigning spins and parities will be discussed in the next paper.

#### ACKNOWLEDGMENTS

We wish to thank Dr. R. Gunnink of the Lawrence Radiation Laboratory in Livermore for permission to quote the transitions observed in his work with a Compton-suppressed system, and Dr. R. Henck for private communication of his results. The helpful comments of Dr. N. R. Johnson and Dr. A. V. Ramayya also are gratefully acknowledged.

<sup>22</sup> H. K. Carter, W. H. Brantley, J. C. Manthuruthil, and J. J. Pinajian, in Proceedings of the Conference on Radioactivity in Nuclear Spectroscopy, 1969 (unpublished).